All-optical pulse compression of broadband microwave signal based on stimulated Brillouin scattering

Xin Long,[1] Weiwen Zou,[1,2,*] and Jianping Chen[1,2]

[1]*State Key Laboratory of Advanced Optical Communication Systems and Networks, Department of Electronic Engineering, Shanghai Jiao Tong University, Shanghai 200240, China*
[2]*Shanghai Key Lab of Navigation and Location Services, Shanghai Jiao Tong University, Shanghai 200240, China*
[*]*wzou@sjtu.edu.cn*

Abstract: Pulse compression processing based on stimulated Brillouin scattering (SBS) in an optical fiber is theoretically and experimentally demonstrated. Broadband microwave signal is electro-optically modulated onto the pump lightwave that is launched into one end of the fiber. Acoustic wave in the fiber inherits the amplitude and phase information of the pump lightwave and thus the coupling between the acoustic wave and pump lightwave leads to the auto-correlated process of the pump lightwave as well as the modulated microwave signal. Derivation of the SBS coupling equations shows that the short-pulse probe lightwave amplified by the pump lightwave possesses the nature of auto-correlation formula. All-optical pulse compression of the broadband microwave signal is implemented after a subtraction between the detected probe pulse with and without SBS. A proof-of-concept experiment is carried out. The pulse compression of a linear frequency-modulated microwave signal with 1 GHz sweep range at the carrier frequency of 4.3 GHz is successfully realized, which well matches the theoretical analysis.

OCIS codes: (070.1170) Analog optical signal processing; (190.0190) Nonlinear optics; (290.5900) Scattering, stimulated Brillouin.

References and links

1. C. E. Cook, "Pulse compression-key to more efficient radar transmission," in *Proceedings of the Institute of Radio Engineers* (IEEE, 1960), pp. 310–316.
2. E. C. Farnett and G. H. Stevens, "Pulse compression radar," in *Radar Handbook 2*, M. I. Skolnik, ed. (McGraw-Hill, 1990), Ch. 10.
3. D. R. Morgan, "Surface acoustic wave devices and applications," Ultrasonics **11**(3), 121–131 (1973).
4. R. E. Milleit, "A matched-filter pulse-compression system using a nonlinear FM waveform," in *IEEE Transactions on Aerospace and Electronic Systems*, (IEEE, 1970), pp. 73–78.
5. E. Mosca, "Sidelobe reduction in phase-coded pulse compression radars (corresp.)," in *IEEE Transactions on Information Theory* (IEEE, 1967), pp. 131–134.
6. P. Ghelfi, F. Scotti, F. Laghezza, and A. Bogoni, "Photonic generation of phase-modulated RF signals for pulse compression techniques in coherent radars," J. Lightwave Technol. **30**(11), 1638–1644 (2012).
7. R. Walden, "Analog-to-digital conversion in the early twenty-first century," in *Wiley Encyclopedia of Computer Science and Engineering* (Wiley, 2008), pp. 126–138.
8. J. Yao, "Microwave photonics," J. Lightwave Technol. **27**(3), 314–335 (2009).
9. J. Capmany and D. Novak, "Microwave photonics combines two worlds," Nat. Photonics **1**(6), 319–330 (2007).
10. P. Ghelfi, F. Laghezza, F. Scotti, G. Serafino, A. Capria, S. Pinna, D. Onori, C. Porzi, M. Scaffardi, A. Malacarne, V. Vercesi, E. Lazzeri, F. Berizzi, and A. Bogoni, "A fully photonics-based coherent radar system," Nature **507**(7492), 341–345 (2014).
11. H. Zhang, W. Zou, and J. Chen, "Generation of a widely tunable linearly chirped microwave waveform based on spectral filtering and unbalanced dispersion," Opt. Lett. **40**(6), 1085–1088 (2015).
12. J. Sun, Y. Dai, X. Chen, Y. Zhang, and S. Xie, "Stable dual-wavelength DFB fiber laser with separate resonant cavities and its application in tunable microwave generation," IEEE Photonics Technol. Lett. **18**(24), 2587–2589 (2006).

#256323 Received 23 Dec 2015; revised 23 Feb 2016; accepted 25 Feb 2016; published 1 Mar 2016

13. Y. Li, A. Rashidinejad, J.-M. Wun, D. E. Leaird, J.-W. Shi, and A. M. Weiner, "Photonic generation of W-band arbitrary waveforms with high time-bandwidth products enabling 3.9 mm range resolution," Optica **1**(6), 446–454 (2014).
14. L. Goldberg, R. D. Esman, and K. J. Williams, "Generation and control of microwave signals by optical techniques," in *Optoelectronics* (IEEE, 1992), pp. 288–295.
15. W. Zou, S. Yang, X. Long, and J. Chen, "Optical pulse compression reflectometry: proposal and proof-of-concept experiment," Opt. Express **23**(1), 512–522 (2015).
16. J. Zhang and J. Yao, "Time-stretched sampling of a fast microwave waveform based on the repetitive use of a linearly chirped fiber Bragg grating in a dispersive loop," Optica **1**(2), 64–69 (2014).
17. D. Marpaung, B. Morrison, M. Pagani, R. Pant, D.-Y. Choi, B. Luther-Davies, S. J. Madden, and B. J. Eggleton, "Low-power, chip-based stimulated Brillouin scattering microwave photonic filter with ultrahigh selectivity," Optica **2**(2), 76–83 (2015).
18. G. C. Valley, "Photonic analog-to-digital converters," Opt. Express **15**(5), 1955–1982 (2007).
19. A. Khilo, S. J. Spector, M. E. Grein, A. H. Nejadmalayeri, C. W. Holzwarth, M. Y. Sander, M. S. Dahlem, M. Y. Peng, M. W. Geis, N. A. DiLello, J. U. Yoon, A. Motamedi, J. S. Orcutt, J. P. Wang, C. M. Sorace-Agaskar, M. A. Popović, J. Sun, G. R. Zhou, H. Byun, J. Chen, J. L. Hoyt, H. I. Smith, R. J. Ram, M. Perrott, T. M. Lyszczarz, E. P. Ippen, and F. X. Kärtner, "Photonic ADC: overcoming the bottleneck of electronic jitter," Opt. Express **20**(4), 4454–4469 (2012).
20. G. Yang, W. Zou, X. Li, and J. Chen, "Theoretical and experimental analysis of channel mismatch in time-wavelength interleaved optical clock based on mode-locked laser," Opt. Express **23**(3), 2174–2186 (2015).
21. G. P. Agrawal, *Nonlinear Fiber Optics* (Academic, 2007).
22. Z. Zhu, D. J. Gauthier, and R. W. Boyd, "Stored light in an optical fiber via stimulated Brillouin scattering," Science **318**(5857), 1748–1750 (2007).
23. W. Zou, Z. He, and K. Hotate, "Complete discrimination of strain and temperature using Brillouin frequency shift and birefringence in a polarization-maintaining fiber," Opt. Express **17**(3), 1248–1255 (2009).
24. X. Bao and L. Chen, "Recent progress in Brillouin scattering based fiber sensors," Sensors (Basel) **11**(4), 4152–4187 (2011).
25. K. Y. Song, M. Herráez, and L. Thévenaz, "Observation of pulse delaying and advancement in optical fibers using stimulated Brillouin scattering," Opt. Express **13**(1), 82–88 (2005).
26. Y. Okawachi, M. S. Bigelow, J. E. Sharping, Z. Zhu, A. Schweinsberg, D. J. Gauthier, R. W. Boyd, and A. L. Gaeta, "Tunable all-optical delays via Brillouin slow light in an optical fiber," Phys. Rev. Lett. **94**(15), 153902 (2005).
27. L. Zhang, L. Zhan, K. Qian, J. Liu, Q. Shen, X. Hu, and S. Luo, "Superluminal propagation at negative group velocity in optical fibers based on Brillouin lasing oscillation," Phys. Rev. Lett. **107**(9), 093903 (2011).
28. N. Levanon and E. Mozeson, *Radar Signals* (W. John and Sons, 2004), Ch. 4.
29. K. Y. Song, W. Zou, Z. He, and K. Hotate, "All-optical dynamic grating generation based on Brillouin scattering in polarization-maintaining fiber," Opt. Lett. **33**(9), 926–928 (2008).
30. B. J. Eggleton, C. G. Poulton, and R. Pant, "Inducing and harnessing stimulated Brillouin scattering in photonic integrated circuits," Adv. Opt. Photonics **5**(4), 536–587 (2013).

1. Introduction

Pulse compression raised up in 1960s is a key signal processing technique to realize better spatial resolution and higher signal-to-noise ratio in the radar field [1]. It is in principle a process that the received broadband signal correlates with the conjugated signal. Many efforts have been made to improve the devices and waveforms in pulse compression system [2]. Among them are the digital processing and surface-wave processing that allow the implementation of more complicated signal waveforms [3–5]. As modern coherent radar systems utilize ultrahigh frequency signals with much larger bandwidth, the signal processing and phase stability have become significant issues to be concerned [6]. For instance, the matched filtering process of the microwave signal for modern coherent radar application is always required after the digitization [1, 2]. It leads to a big challenge for analog-to-digital conversion (ADC) that should provide sufficient analogue bandwidth, ultra-high sampling rate, and great sampling resolution (also called the effective number of bits) [7]. The pulse duration of the radar's microwave signal is sufficiently long so as to increase its transition distance, which sharply increases the depth and speed difficulty of digital storage. Therefore, the huge bit-rates of the digitized signal due to the broad bandwidth and long pulse duration of the microwave signal make ADC, digital storage, and signal processing more and more challengeable.

Microwave photonics [8–10] combines the merits in microwave and photonic techniques and enables the generation [11–13], control [14], and processing [15–17] of broadband

#256323 Received 23 Dec 2015; revised 23 Feb 2016; accepted 25 Feb 2016; published 1 Mar 2016

microwave signals with high phase stability. To overcome the bandwidth limit of the electronic ADC, several types of photonic ADCs [18–20] have been proposed. However, photonics ADCs can't reduce the requirement of digital storage and signal processing. Thus, an all-optical scheme that achieves auto-correlation process before digitization is significantly desired. To the best of our knowledge, the photonics-based analogue matched filtering for the pulse compression of the broadband microwave signal has not been reported so far. In optical fibers, stimulated Brillouin scattering (SBS) is in principle three-wave interaction among the pump lightwave, the counter-propagated probe lightwave, and the acoustic wave [21]. The acoustic wave is excited due to the electro-striction effect when the pump and probe lightwaves interact in the fiber. Such a property has been successfully utilized in other applications to signal storage [22], fiber-optic sensors [23, 24], and slow light [25–27].

In this paper, we demonstrate the SBS-based pulse compression for all-optical characterization of broadband microwave signals. When the acoustic wave is induced by the coupling between the pump and probe lightwaves and the electro-striction effect, it inherits the amplitude and phase information of the lightwaves. In this way, the time delay and amplitude conjugation conditions that are necessary for the matched filtering are automatically satisfied during the re-coupling between this acoustic wave and pump lightwave. Thus, the pump lightwave carrying the microwave signal amplifies the short-pulse probe lightwave via the acoustic wave. Consequently, the pulse compression is implemented by direct detection of the probe pulse with and without SBS, which is short in time and thus significantly reduces the difficulty of digital storage and signal processing. Experiment is conducted to verify the feasibility of the pulse compression of linear frequency modulated (LFM) pulses with 1 μs pulse duration and 1 GHz sweep range at 4.3 GHz carrier frequency. The range resolution of compressed LFM signal is 0.88 ns, which is in good agreement with the ideal auto-correlation of the LFM pulse.

2. Principle

Without loss of generality, we assume that the pump and probe lightwaves are launched into the two ends of an optical fiber at $z = 0$ (near end) and $z = L$ (far end), respectively. L denotes the length of the fiber. The coupling equations describing the SBS interaction in the fiber is given by [21]:

$$\left(\frac{\partial}{\partial t}+\Gamma\right)Q(z,t)=-ig_1E_P(z,t)E_S^{*}(z,t), \tag{1}$$

$$\left(\frac{\partial}{\partial z}+\frac{1}{v}\frac{\partial}{\partial t}\right)E_P(z,t)=ig_2E_S(z,t)Q(z,t), \tag{2}$$

$$\left(\frac{\partial}{\partial z}-\frac{1}{v}\frac{\partial}{\partial t}\right)E_S(z,t)=-ig_2E_P(z,t)Q^{*}(z,t), \tag{3}$$

where g_1 and g_2 are electro-strictive parameters. v denotes the light velocity in the fiber. $Q(z,t)$, $E_P(z,t)$ and $E_S(z,t)$ represent slowly-varying envelopes of the acoustic wave, pump and probe fields at position z and time t, respectively. $\Gamma = 1/(2\tau_p) + i(\Delta\omega-\omega_B)$ is the detuning and damping coefficient with τ_p representing the phonon lifetime and $\Delta\omega$ corresponding to beat frequency between pump and probe. ω_B is the Brillouin frequency shift (BFS).

Equations (2) and (3) can be modified as homogeneous when weak probe lightwave is injected, so that both the pump and probe fields can be expressed by:

$$E_P(z,t)=E_{P0}\left(t-\frac{z}{v}\right), \tag{4}$$

#256323 Received 23 Dec 2015; revised 23 Feb 2016; accepted 25 Feb 2016; published 1 Mar 2016

$$E_S(z,t) = E_{S0}\left(t - \frac{L-z}{v}\right), \tag{5}$$

where $E_{P0}(t)$ and $E_{S0}(t)$ denote the complex envelope function for the injected pump and probe lightwaves, respectively.

According to Eq. (4) and Eq. (5), the solution to Eq. (1) is given by:

$$Q(z,t) = -ig_1\int_{-\infty}^{t} E_{P0}\left(\tau - \frac{z}{v}\right)E_{S0}^{*}\left(\tau - \frac{L-z}{v}\right)e^{-\Gamma(t-\tau)}d\tau, \tag{6}$$

which shows that the acoustic wave (Q) inherits the amplitude and phase information of the lightwaves (E_{P0} and E_{S0}).

The SBS process and the excitation of the acoustic wave are schematically illustrated in Fig. 1. All the symbols defined above are presented in Fig. 1(a). As shown in Fig. 1(b), an LFM pulse is modulated onto the pump lightwave (E_P) at $z = 0$ and the probe lightwave at $z = L$ is a short pulse (E_S). The probe pulse is downshifted in frequency from the pump lightwave and the downshifted frequency is equal to the BFS in the fiber. Since the modulated pump lightwave contains a broadband LFM pulse, the bandwidth of the probe lightwave should be wide enough. When they meet each other, the acoustic wave (Q) is generated at the same frequency as the BFS [see Fig. 1(c)]. As time goes by, 'new' phonons are excited along the fiber while 'old' ones attenuate and disappear rapidly [see Fig. 1(d)]. Finally, as depicted in Fig. 1(d), the amplified probe lightwave (E_S') is detected at $z = 0$ [see Fig. 1(e)].

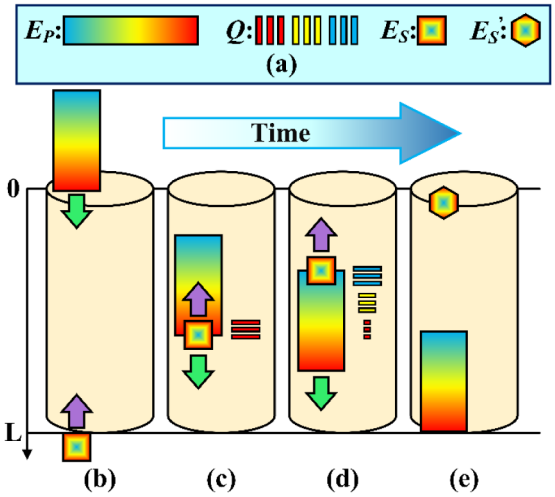

Fig. 1. The SBS process and the excitation of the acoustic wave. (a) Illustration for the symbols. E_P: pump lightwave, which is modulated by an LFM pulse. Q: acoustic wave. E_S: short-pulse probe lightwave. E_S': received probe pulse. (b) Pump lightwave is injected at $z = 0$ while the counter-propagating probe lightwave is launched at $z = L$. (c) The first time when the two lightwaves meet each other and acoustic wave is generated. (d) 'New' acoustic waves are stimulated while 'old' ones last for a lifetime and disappear finally. (e) Amplified probe lightwave is detected at the near end of the fiber.

Substituting Eqs. (4-6) into Eq. (3), the electric field of the detected probe lightwave, $E_S'(t)$, can be expressed by:

$$E_S'(t+T) = \frac{g_B v}{8\tau_p}\left\{E_{S0}(t) \otimes \left[u(t)\, y_P(t) e^{-\Gamma^* t}\right]\right\} + E_{S0}(t), \tag{7}$$

#256323 Received 23 Dec 2015; revised 23 Feb 2016; accepted 25 Feb 2016; published 1 Mar 2016

where $g_B = 4g_1g_2\tau_p$ is the Brillouin gain coefficient, $T = L/v$ represents the period needed for optical light to travel through the fiber, the symbol of ⊗ denotes the convolution algebra, and $u(t)$ is the unit step function. $y_P(t)$ in Eq. (7) is given by:

$$y_P(t) = E_{P0}(t) \otimes E_{P0}^{*}(-t), \tag{8}$$

which corresponds to the auto-correlation formula of the pump field $E_{P0}(t)$ that is modulated by the broadband microwave signal.

Note that $E_S'(t + T)$ and $E_{S0}(t)$ represent the probe field at near end with and without the pump lightwave running into the fiber, their subtraction is needed to extract the term of $y_P(t)$ from $E_S'(t + T)$. For a direct detection system, the detected voltage signal is proportional to the optical power of the probe lightwave. Thus the signal after subtraction can be expressed as follows:

$$s(t+T) \propto \left|E_S'(t+T)\right|^2 - \left|E_{S0}(t)\right|^2 = \left|\Delta E_S(t)\right|^2 + 2\,\mathrm{Re}\left\{\Delta E_S(t) E_{S0}^{*}(t)\right\}, \tag{9}$$

where $\Delta E_S(t) = E_S'(t + T) - E_{S0}(t)$ represents the Brillouin gain factor and $Re\{\cdot\}$ denotes real part of the complex signal. $s(t + T)$ is divided into two parts in terms of different time. When t is smaller than the probe pulse duration τ_S, Brillouin gain can be considered as a small signal and thus the term of $|\Delta E_S(t)|^2$ in Eq. (9) can be ignored [see Eq. (10)]. Whereas t is larger than τ_S, the term of $2Re\{\Delta E_S(t)\ E_{S0}^{*}(t)\}$ can be neglected as a result of $E_{S0}(t) \approx 0$ for a high extinction ratio (ER) of the short-pulse probe lightwave [see Eq. (11)].

$$s(t+T) \propto 2\,\mathrm{Re}\left\{\Delta E_S(t) E_{S0}^{*}(t)\right\}, \quad \text{when } t < \tau_S, \tag{10}$$

$$s(t+T) \propto \left|\Delta E_S(t)\right|^2, \quad \text{when } t \geq \tau_S, \tag{11}$$

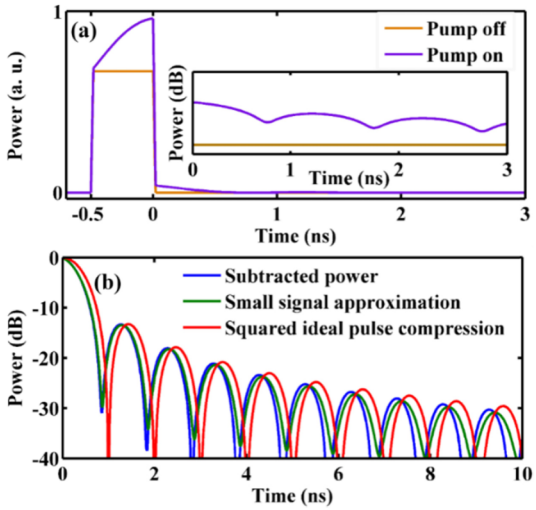

Fig. 2. Simulation results for the pulse compression based on the SBS process. The pump lightwave is modulated by an LFM pulse with 1 GHz sweep range and the probe lightwave is a short pulse with 0.5 ns duration. (a) The detected probe power with and without the pump lightwave. The inset shows the log scale of the vertical axis. (b) The subtracted power is compared to the small signal approximation and the squared ideal pulse compression.

Simulation result is depicted in Fig. 2. A 1 μs LFM pulse with 1 GHz sweep range is modulated onto a continuous-wave pump lightwave, and a 0.5 ns pulse with 40 dB ER is used as the probe lightwave. The BFS is set uniform along the fiber and τ_p = 10 ns. Figure 2(a)

#256323 Received 23 Dec 2015; revised 23 Feb 2016; accepted 25 Feb 2016; published 1 Mar 2016

shows the comparison of the detected probe power with and without the pump lightwave. The above-mentioned two parts in the amplified probe power can be identified. One corresponding to $t < \tau_S$ is accumulated from the probe lightwave and is not useful for this study. Whereas the other at the rear of the pulse corresponds to the desired pulse compression of the LFM pulse. After the horizontal coordinate adjustment in Fig. 2(a), these two parts are separated by $t = 0$. Figure 2(b) shows the subtracted signal defined in Eq. (9). It is compared with the small signal approximation given by the term of $|\Delta E_S(t)|^2$ in Eq. (11) and the squared ideal pulse compression of the LFM pulse $|y_P(t)|^2$ defined in Eq. (8). The ideal pulse compression of the broadband microwave signal matches well the small signal approximation as well as the directly subtracted power. For an LFM pulse with large time-wavelength product, the range resolution (R) for its pulse compression is defined as the width between the peak and the first null, which approximately equals to the reciprocal of the bandwidth (B) of the LFM pulse, as follows [28]:

$$R \approx \frac{1}{B}. \tag{12}$$

As we can see from Fig. 2(b), the range resolutions R for the small signal approximation and the subtracted power equal to each other, that is, 0.86 ns, which approximately equals to that of the ideal pulse compression (1 ns). The possible attribution to the tiny difference will be demonstrated in the Discussion session.

3. Experimental details

Figure 3 depicts the experimental setup. Light from a 1550 nm distributed-feedback laser (DFB-LD, NEL NLK1C6DAAA) is split into two paths by a 1:1 fiber coupler. The upper branch is used as the pump lightwave. Through an electro-optic modulator (EOM1), the pump lightwave is modulated by the input microwave signal to be processed. The lower branch is modulated by another EOM2 (Eospace, AX-6K5-10-PFU-PFUP-R4). To generate the frequency difference between these two branches, a single sideband modulator (SSBM) is additionally used in the lower branch. The first lower sideband of the modulated signal after SSBM is selected and thus the beat frequency between the pump and probe lightwaves equals to the BFS of the optical fiber. Polarization controllers (PC1, PC2, and PC3) are used to optimize the light polarizations before the modulators. PC4 and PC5 ensure the maximum SBS interaction in a standard single-mode optical fiber (SMF). A circulator is used for the isolation of the pump lightwave and transmission of the amplified probe lightwave. A photo-detector (PD) converts the detected probe power into the electric signal, namely the compressed signal.

The output power of the DFB-LD is around 13 dBm and those of two branches for the two modulators (EOM1 and EOM2) are around 10 dBm, which are close to the saturation powers of the modulators. Thus, there is no need for additional amplification before the modulators. Erbium-doped fiber amplifiers (EDFA1 and EDFA2) are utilized to compensate the power loss caused by the modulators and also control the optical powers of the pump and probe lightwaves launched into the fiber.

As a proof-of-concept experimental verification, the pump lightwave is modulated by an LFM pulse which is generated via a voltage-controlled oscillator (VCO, Mini-circuits ZX95-5400-S +) and an RF amplifier (Mini-circuits ZX60-542LN-S +). The LFM pulse's duration is set to be 1 μs and its frequency is linearly swept. Since the frequency of the pump lightwave is linearly modulated, a 0.5 ns pulse with sufficient bandwidth is modulated on the probe lightwave so that the beat frequency between the pump and probe lightwaves meeting at different positions of the 200-meter-long SMF maintains to cover 10.813 GHz (i.e. the BFS of the SMF). The driving frequency for the SSBM is set to be 6.513 GHz. The average power of the pump and probe lightwaves before entering the SMF are 20 dBm and 10 dBm, respectively. Each experimental result is acquired after 1000-times average.

#256323 Received 23 Dec 2015; revised 23 Feb 2016; accepted 25 Feb 2016; published 1 Mar 2016

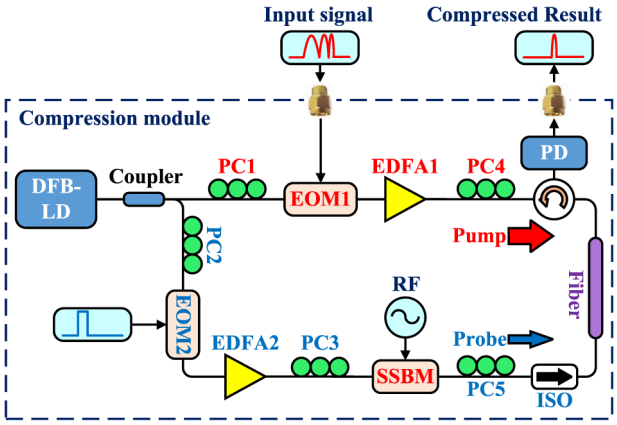

Fig. 3. Experimental setup for pulse compression of the broadband microwave frequency based on SBS process. DFB-LD: distributed-feedback laser. PC: polarization controller. EOM: electro-optic modulator. EDFA: erbium-doped fiber amplifier. ISO: isolator. SSBM: single sideband modulator. PD: photo-detector.

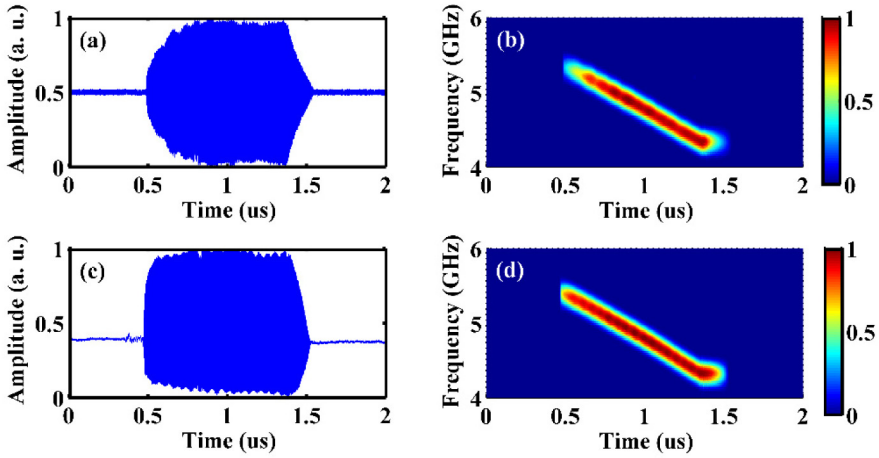

Fig. 4. Time profile (a) and short-time Fourier transform (b) of the LFM pulse to be processed. The LFM pulse has 1 μs duration and 1 GHz sweep range. Time profile (c) and short-time Fourier transform (d) of the pump lightwave that is modulated by the LFM pulse.

Figure 4 presents the time profiles and short-time Fourier transform of the LFM pulse before and after the EOM1. It is shown that the pulse durations of these LFM are around 1 μs and their frequencies sweep linearly from around 5.3 GHz to 4.3 GHz. The bandwidth-to-carrier ratio of the LFM pulse is 23.3%. Due to the nonlinearity of the EOM1, there is somewhat distortion (such as the offset) of the time profile after the EOM1. However, the corresponding short-time Fourier transforms are similar with each other.

By turning on and off the EDFA1, the detected probe powers with and without the Brillouin gain are obtained and illustrated in Fig. 5(a). The subtracted voltage of these two powers at the rear of the pulse is proportional to the term of $|\Delta E_S(t)|^2$ that is defined by Eq. (9). Figure 5(b) depicts the squared ideal pulse compressions of the LFM pulses before and after the EOM1 [see Figs. 4(a) and 4(c)] and the subtraction of the two probe powers shown in Fig. 5(a). As mentioned above, the nonlinearity of the modulator distorts more or less the LFM pulse after modulation. The subtracted voltage is in better agreement, especially in the mainlobe and the first sidelobe, with the squared ideal pulse compressions of the LFM pulse after modulation rather than that of the microwave signal itself.

#256323 Received 23 Dec 2015; revised 23 Feb 2016; accepted 25 Feb 2016; published 1 Mar 2016

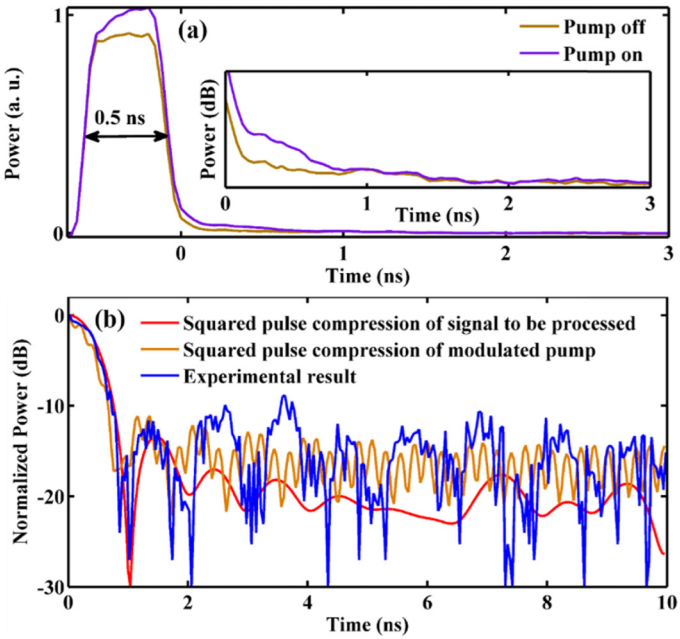

Fig. 5. Experiment results for the pulse compression based on the SBS process. (a) The detected probe power with and without the pump lightwave injected. (b) The pulse compression achieved by the subtraction in (a) is compared with the squared ideal pulse compressions of the LFM pulses before and after the modulation [see Figs. 4(a) and 4(c)].

The range resolution R (or compressed width) of the experimental curve is about 0.88 ns, which agrees well with the theoretical value shown in Fig. 2(b) whereas a little bit smaller than the reciprocal of 1 GHz sweep range (1 ns). The physical reason will be presented in Discussion section. Moreover, the range resolution R of the LFM pulse with different B is depicted in Fig. 6. It shows a clear inverse relation between R and B of the LFM pulse, which matches well Eq. (12).

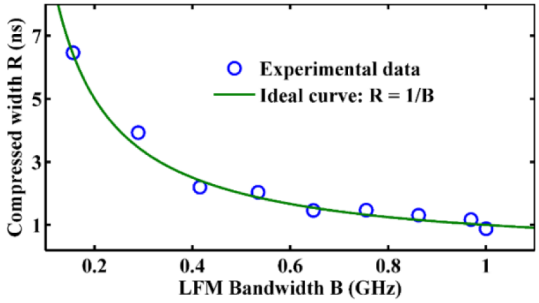

Fig. 6. The full width of the compressed mainlobe as a function of the sweeping bandwidth of the LFM pulse.

4. Discussion

As can be seen from Figs. 2(b) and 5(b), there are more or less mismatches in the simulation and experiment. Comparison among Eq. (7), Eq. (8), and Eq. (9) shows that the term of $\Delta E_S(t)$ is just an approximation of $y_P(t)$. When $t > 0$, $\Delta E_S(t)$ is exponentially reduced and the condition of $|\Delta E_S(t)|^2 >> 2Re\{\Delta E_S(t)E_{S0}^*(t)\}$ is somehow broken so that the term $2Re\{\Delta E_S(t)E_{S0}^*(t)\}$ in Eq. (9) cannot be ignored. To further overcome this influence, a short-pulse probe lightwave with much higher ER might work better. In the experiment, the

#256323 Received 23 Dec 2015; revised 23 Feb 2016; accepted 25 Feb 2016; published 1 Mar 2016

sidelobes of the compressed pulse by the SBS based method can be roughly observed [see Fig. 5(b)]. However, the thermal noise of the photo-detector and amplitude/phase noise of the laser diode distorts the detected probe power and thus influences the compressed pulse (especially, the weak sidelobes). Moreover, the two EDFAs in the pump and probe lightwaves induce more or less pulse distortion and ER reduction. In the future work, sophisticated study of system noise influence and better design of EDFAs for short/broadband pulse amplification are required.

In Eq. (7), the convolution between $E_{S0}(t)$ and $u(t)y_P(t)\exp(-\Gamma^* t)$ brings in distortion to the compressed term of $|\Delta E_S(t)|^2$. The probe pulse duration τ_s is one of the key parameters that determines this distortion. Figure 7(a) shows the simulation result of $|\Delta E_S(t)|^2$ with different values of τ_s. The sweep range of the LFM pulse is 1 GHz and τ_p = 10 ns. When τ_s increases, the mainlobes and sidelobes of $|\Delta E_S(t)|^2$ become narrow and the dips among the sidelobes gradually disappear. It attributed to the discrepancy in the mainlobe of Fig. 5(b). If a 0.1 ns short-pulse probe lightwave is used, a better result of the all-optical pulse compression based on the SBS is expectable. However, a shorter probe pulse sharply weakens the Brillouin gain as well as the subtracted voltage between the pump lightwave turned on and off. In the future work, a shorter pulse generator and amplifier with better performance is needed to verify the numerical analysis.

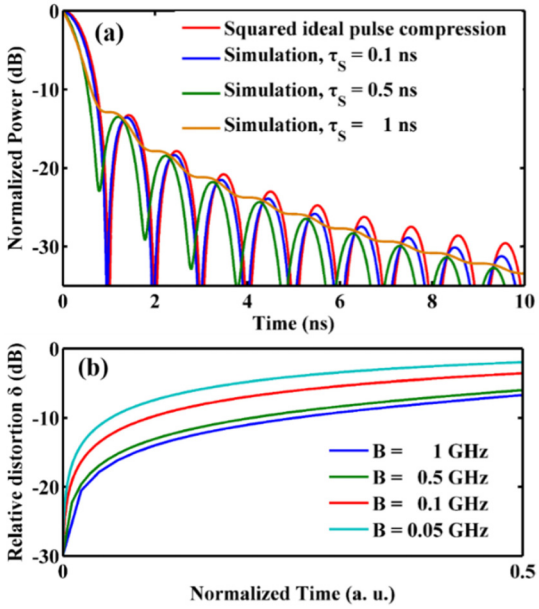

Fig. 7. Analysis on the distortions that induced by the pulse duration (τ_S) of the probe lightwave and the phonon lifetime. (a) Comparison between the squared pulse compression of $|y_P(t)|^2$ and subtracted signal of $|\Delta E_S(t)|^2$ with different τ_S. (b) Relative distortions caused by the phonon lifetime τ_p for different LFM pulse bandwidths B. Horizontal coordinate is normalized by the factor of $1/B$.

Besides, the phonon lifetime τ_p (which is usually 10 ns) also influences the performance of the all-optical pulse compression. This is because the term of $\exp(-\Gamma^* t)$ or $\exp[-t/(2\tau_p)]$ is multiplied with the compressed pulse of $y_P(t)$ in Eq. (7). The accuracy of the pulse compression via the SBS based method is ensured if the range resolution R of the compressed pulse is within several nanoseconds. According to Eq. (12), the bandwidth B of the microwave signal to be processed is also influenced.

To quantitatively characterize this influence, the relative distortion is defined as follows:

#256323 Received 23 Dec 2015; revised 23 Feb 2016; accepted 25 Feb 2016; published 1 Mar 2016

$$\delta = \left[\left| y_P(t) \right|^2 - \left| \Delta E_S(t) \right|^2 \right] \Big/ \left| y_P(t) \right|^2 . \quad (13)$$

Figure 7(b) depicts the simulation results of the relative distortion as a function of the bandwidth (B) of the LFM pulse. A 0.1 ns probe pulse with infinite ER and τ_p = 10 ns are assumed. The horizontal coordinate (time) is normalized by the factor of $1/B$ so as to compare the relative distortion among all the compressed mainlobes of different LFM pulses. It is shown that the LFM pulses with higher B suffer less distortion to the pulse compression. In other words, the all-optical pulse compression proposed in this work is essentially advantageous for broadband microwave signal.

5. Conclusion

We theoretically and experimentally demonstrate the SBS based pulse compression for a broadband microwave signal. During the interaction between the pump lightwave and acoustic wave in the SBS process, the time delay and amplitude conjugation conditions for matched filtering are automatically satisfied. This is because the acoustic wave inherits the amplitude and phase information of the microwave signal that is modulated onto the pump lightwave. Theoretical derivation indicates that the auto-correlation of the microwave signal appears in the formula of the amplified probe field. Thus, all-optical pulse compression is implemented by subtraction of the detected probe lightwave with the pump lightwave from that without pump lightwave. Under the small signal approximation, the subtraction equals to the squared pulse compression of the microwave signal. A proof-of-concept experiment is carried out to validate the pulse compression of an LFM pulse with 1 μs pulse duration and 1 GHz sweep range. The resolution of compressed signal of the broadband microwave signal via the SBS based pulse compression is about 0.88 ns, which is in a reasonable agreement with the auto-correlation of the LFM pulse.

Moreover, factors that introduce the discrepancies between the SBS based pulse compression and the ideal one are analyzed, which points out the future efforts to avoid the distortions that caused by the noise, pulse duration, and phonon lifetime. For instance, the use of the optical fiber with high nonlinearity and Brillouin gain is a possible way. Establishing and analyzing of the noise model is also required for further theoretical study. If one wants to restore the phase information of the microwave signal, the recently raised Brillouin dynamic grating technique [23, 29] is a possible scheme since it can separate the writing and reading of the acoustic wave. However, in this study, the phase information of the signal to be processed is lost during the re-coupling between the acoustic wave and pump/probe lightwave. Besides, referred to the development of the SBS integrated photonic circuits [30], the SBS interaction might be realized in a chip-scale device instead of the long optical fiber, which will miniaturize the whole system and make it more suitable for practical applications.

Acknowledgments

This work was partially supported by National Natural Science Foundation of China (Grant Nos. 61571292 and 61535006) and by the State Key Lab Project of Shanghai Jiao Tong University (Grant Nos. 2014ZZ03016).

#256323 Received 23 Dec 2015; revised 23 Feb 2016; accepted 25 Feb 2016; published 1 Mar 2016